The 11th International Symposium on Wireless Personal Multimedia Communications (WPMC 2008)

# UPLINK CAPACITY OF A SINGLE-CARRIER MULTI-USER MIMO MULTIPLEXING IN A FREQUENCY-SELECTIVE CHANNEL

Takahiro CHIBA, Kazuaki TAKEDA and Fumiyuki ADACHI
Dept. of Electrical and Communication Eng., Tohoku University
6-6-05 Aza-Aoba, Aramaki, Aoba-ku, Sendai, 980-8579, Japan

## ABSTRACT

Multi-user single-carrier (SC) MIMO multiplexing has been attracting a lot of attention due to its low peak-to-average power ratio (PAPR). As the transmission rate increases, the channel becomes frequency-selective and the bit error rate (BER) performance degrades significantly due to inter-symbol interference (ISI). Frequency-domain equalization (FDE) provides a good BER performance since the frequency diversity gain can be obtained. In this paper, we evaluate, by computer simulation, the uplink capacity of multi-user SC-MIMO multiplexing using FDE in a frequency-selective fading channel. Zero-forcing detection (ZFD) and minimum mean square error detection (MMSED) are considered. The uplink capacity is found from the complimentary cumulative distribution function (CCDF) of the local average BER, obtained by computer simulation. It is shown that larger uplink capacity can be achieved in a frequency-selective fading channel rather than in a frequency-nonselective fading channel and that almost the same capacity is obtained by ZFD and MMSED. It is also shown that ZFD and MMSED can provide almost 1.3 times larger uplink capacity than MMSE-FDE+antenna diversity reception using 8-element receive antenna array.

## I. INTRODUCTION

High-speed data services are strongly demanded in next-generation mobile communication systems [1]. The available bandwidth is limited. Multiple-input multiple-output (MIMO) multiplexing is one of the promising techniques. In MIMO multiplexing, different data are simultaneously transmitted from different transmit antennas with the same carrier frequency. At a receiver, a superposition of different antennas' signals is received and therefore, an efficient signal detection scheme is necessary.

Broadband wireless channel consists of many propagation paths having different time delays, resulting in frequency-selective fading. This fading channel causes severe inter-symbol interference for single-carrier (SC) transmission [2]. A joint use of MIMO multiplexing and orthogonal frequency division multiplexing (OFDM) has been gaining an increasing popularity due to its robustness against the channel frequency-selectivity [3]. OFDM, however, has a problem of large peak-to-average power ratio (PAPR). Frequency-domain equalization (FDE) [4] provides a good bit error rate (BER) performance of SC transmissions [5]. SC transmission with FDE has been drawing much attention for the uplink transmission owing to its lower PAPR [6].

MIMO multiplexing, where each transmit antenna is allocated to a different user, is called multi-user MIMO multiplexing [7]. In cellular mobile communication systems, the same carrier frequency is reused at geographically separated base stations (BSs) to efficiently utilize the limited bandwidth [8]. Many works on the channel capacity of multi-user MIMO have been reported assuming single-cell environment [9, 10]. So far, there has been only a few works on the link capacity of multi-user SC-MIMO in a cellular system.

In this paper, we evaluate, by computer simulation, the cellular uplink capacity of multi-user SC-MIMO multiplexing with FDE in a frequency-selective fading channel. For signal detection, we consider zero-forcing detection (ZFD) and minimum mean square error detection (MMSED).

## II. INTERFERENCE MODEL

Uplink multi-user MIMO multiplexing allows multiple users to simultaneously communicate without reducing the transmission data rate. Each user is assumed to have single transmit antenna. $U$ users are simultaneously transmitting their data in each cell by using the same carrier frequency. A superposition of $U$ transmitted signals is received at each BS, which is assumed to have $N_r$ ($\geq U$) receive antennas.

In the cellular system, the whole channels are divided into a number of channel groups and each channel group is assigned to a different cell [8]. The number $N$ of different channel groups is called the cluster size. The smaller the cluster size becomes, the more channels can be assigned to each cell. Fig. 1 illustrates the interference model for uplink multi-user MIMO multiplexing in a cellular system. The 6 nearest co-channel cells are considered (see Fig. 1). At the BS of interest, a superposition of $U$ users' signals corrupted by the co-channel interference (CCI) from other cells is received. CCI degrades the signal detection quality. CCI can be reduced by increasing the cluster size $N$ (or the distance between the co-channel cells), however, this solution reduces the number of channels per channel group assigned to each BS. Therefore, even if multi-user MIMO multiplexing is used, the frequency utilization efficiency might be degraded.

In this paper, we measure, by the Monte-Carlo simulation, the distribution of local average bit error rate (BER) when multi-user SC-MIMO is used. The outage probability is defined as the probability of the local average BER being larger than the required BER. The link capacity is the maximum number of users per channel group for the given allowable outage probability.

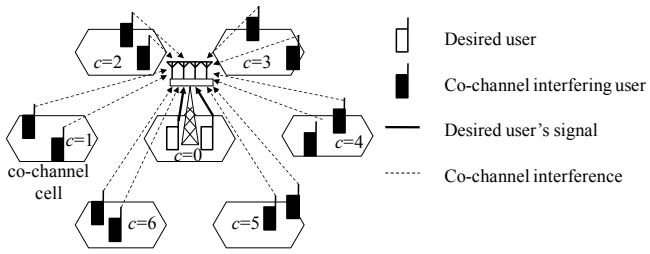


Figure 1. Interference model of uplink multi-user MIMO multiplexing in a cellular system.

## III. MULTI-USER SC-MIMO

### A. Transmission System Model

Fig. 2 illustrates the transmission system model of multi-user SC-MIMO multiplexing with FDE. The uplink transmission in the cell of interest ($c$=0) is considered. At a mobile transmitter, each user's binary data sequence is data-modulated and divided into a sequence of blocks of $N_c$ symbols each. The last $N_g$ symbols in each block are copied and inserted as a cyclic prefix into the guard interval (GI), placed at the beginning of each block, to form a block of $N_g$+$N_c$ symbols (see Fig. 3). Without loss of generality, the transmission of one block is considered, and the transmit timing offset plus maximum propagation time delay among $U$ users of the cell of interest is assumed less than the GI length.

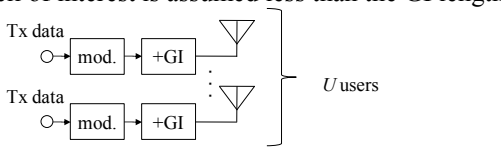


(a) Mobile station transmitter

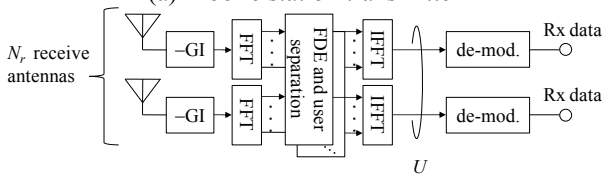


(b) Base station receiver

Figure 2. Transmission system model of multi-user SC-MIMO multiplexing.

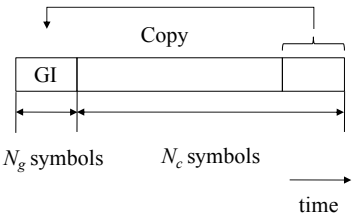


Figure 3. Block structure of the transmitted symbols.

At a BS receiver, a superposition of $U$ users' transmitted signals is received by $N_r$ receive antennas. After the removal of the GI from the received signal, $N_c$-point fast Fourier transform (FFT) is applied to transform the GI-removed received signal into the frequency-domain signal. Joint FDE and user separation is carried out in the frequency-domain. Each user's frequency components are transformed back into time-domain signal block by using $N_c$-point inverse FFT (IFFT) and data demodulation is carried out.

### B. User Separation Method

We use a Gaussian approximation of the CCI. Throughout the paper, symbol-spaced discrete-time signal representation is used.

The GI-inserted symbol block $\bar{\mathbf{s}}_c(t)$ in the vector representation is expressed as

$$\bar{\mathbf{s}}_c(t)=\sqrt{2P}\mathbf{s}_c(t \bmod N_c),\ \ t=-N_g \sim N_c-1, \qquad (1)$$

where, $P$ is the transmit power, and $\mathbf{s}_c(t)=\left[s_{0(c)}(t)\ \ s_{1(c)}(t)\ \ \cdots\ \ s_{U-1(c)}(t)\right]^T, t=0\sim N_c-1$, represents the transmit signal vector from the $U$ users in the $c$-th cell, where $s_{u(c)}(t), u=0\sim U-1$, is the $u$-th user's data-modulated symbol and $(\cdot)^T$ denotes the transposition. Assuming QPSK data-modulation,

$$s_{u(c)}(t)\in\left\{\frac{1}{\sqrt{2}}(1+j),\frac{1}{\sqrt{2}}(1-j),\frac{1}{\sqrt{2}}(-1+j),\frac{1}{\sqrt{2}}(-1-j)\right\}. \qquad (2)$$

The transmitted signal from each user undergoes different frequency-selective fading channel. The channel impulse response between the $u$-th user of the $c$-th cell and the $m$-th receive antenna of the BS of interest ($c$=0) is given by

$$\tilde{h}_{m,u(c)}(t)=\sqrt{r_{u(c)}^{-\alpha}\cdot 10^{-\frac{\eta_{u(c)}}{10}}}\sum_{l=0}^{L-1}h_{m,u(c)}^{(l)}\cdot\delta(t-\tau_l), \qquad (3)$$

where, $r_{u(c)}$, $\eta_{u(c)}$ and $\alpha$ denote the distance between user and BS, the shadowing and the path-loss exponent, respectively. $h_{m,u(c)}^{(l)}$ is the $l$-th path gain with $E\left[\sum_{l=0}^{L-1}\left|h_{m,u(c)}^{(l)}\right|^2\right]=1$, where $E[\cdot]$ denotes the ensemble average operation, and $\tau_l$ represents the $l$-th path time delay. Using the vector representation, the received signal vector can be expressed as

$$\begin{aligned}\mathbf{y}(t)&=\left[y_0(t)\ \ y_1(t)\ \ \cdots\ \ y_{N_r-1}(t)\right]^T\\&=\sum_{l=0}^{L-1}\tilde{\mathbf{h}}_0^{(l)}\cdot\bar{\mathbf{s}}_0(t-\tau_l)+\sum_{c=1}^{6}\sum_{l=0}^{L-1}\left(\tilde{\mathbf{h}}_c^{(l)}\cdot\bar{\mathbf{s}}_c(t-\tau_l)\right)+\mathbf{n}(t),\end{aligned} \qquad (4)$$

where, $\tilde{\mathbf{h}}_c^{(l)}$ is the $N_r\times U$ path gain matrix of the $l$-th path, whose ($m$,$u(c)$)-th elememt is $\tilde{h}_{m,u(c)}^{(l)}=\sqrt{r_{u(c)}^{-\alpha}\cdot 10^{-\frac{\eta_{u(c)}}{10}}}\,h_{m,u(c)}^{(l)}$, and $\mathbf{n}(t)=\left[n_0(t)\ \ n_1(t)\ \ \cdots\ \ n_{N_r-1}(t)\right]^T$ is the $N_r\times 1$ noise vector. The $m$-th element $n_m(t)$ of $\mathbf{n}(t)$ is the additive zero-mean complex white Gaussian variable with variance $2\sigma_n^2$. The first and second terms of (4) are the desired signal and the CCI, respectively.

The received signal $\mathbf{y}(t)$ is then transformed into a frequency-domain signal by using $N_c$-point FFT. The $k$-th frequency components of signal blocks received by $N_r$ receive antennas can be expressed as

$$\mathbf{Y}(k)=\sum_{t=0}^{N_c-1}\mathbf{y}(t)\exp\left(-j\frac{2\pi k}{N_c}t\right) =\widetilde{\mathbf{H}}_0(k)\cdot\mathbf{S}_0(k)+\sum_{c=1}^{6}\left(\widetilde{\mathbf{H}}_c(k)\cdot\mathbf{S}_c(k)\right)+\mathbf{\Pi}(k) \quad (5)$$

where, $\widetilde{\mathbf{H}}_c(k)=\left[\widetilde{\mathbf{H}}_{0(c)}(k)\ \ \widetilde{\mathbf{H}}_{1(c)}(k)\ \cdots\ \widetilde{\mathbf{H}}_{U-1(c)}(k)\right]$, $\mathbf{S}_c(k)=\left[S_{0(c)}(k)\ \ S_{1(c)}(k)\ \cdots\ S_{U-1(c)}(k)\right]^T$, and $\mathbf{\Pi}(k)=\left[\Pi_0(k)\ \ \Pi_1(k)\ \cdots\ \Pi_{N_r-1}(k)\right]^T$ denote the $N_r\times U$ channel gain matrix, the signal vector, and the noise vector, respectively. The $(m,u(c))$-th element $\widetilde{H}_{m,u(c)}(k)$ of $\widetilde{\mathbf{H}}_c(k)$ is given by

$$\widetilde{H}_{m,u(c)}(k)=\sqrt{r_{u(c)}^{-\alpha}\cdot 10^{-\frac{\eta_{u(c)}}{10}}}\cdot H_{m,u(c)}(k), \quad (6)$$

where, $H_{m,u(c)}(k)$ denotes the channel gain. Using (3), $\widetilde{H}_{m,u(c)}(k)$ may be expressed as

$$\widetilde{H}_{m,u(c)}(k)=\sum_{l=0}^{L-1}\widetilde{h}_{m,u(c)}^{(l)}\exp\left(-j\frac{2\pi k}{N_c}l\right). \quad (7)$$

Finally, for signal detection, we consider ZFD and MMSED. The detector output $\widetilde{\mathbf{S}}_0(k)$ is expressed as

$$\widetilde{\mathbf{S}}_0(k)=\mathbf{W}(k)\mathbf{Y}(k), \quad (8)$$

where, $\mathbf{W}(k)=\left[\mathbf{w}_0(k)\ \ \mathbf{w}_1(k)\ \cdots\ \mathbf{w}_{N_r-1}(k)\right]$ represents the $U\times N_r$ detector weight matrix. ZFD estimates the weight that can perfectly restore the transmitted signal. However, MMSED estimates the weight matrix which minimizes the mean square error (MSE) between the transmitted signal and the detector output. The weight matrix expression for both detection methods are given by

$$\mathbf{W}(k)=\begin{cases}\left(\widetilde{\mathbf{H}}_0^H(k)\widetilde{\mathbf{H}}_0(k)\right)^{-1}\widetilde{\mathbf{H}}_0^H(k) & \text{for ZF}\\ \widetilde{\mathbf{H}}_0^H(k)\left(\widetilde{\mathbf{H}}_0(k)\widetilde{\mathbf{H}}_0^H(k)+\dfrac{\sigma_I^2+\sigma_n^2}{P}\right)^{-1} & \text{for MMSE}\end{cases}, \quad (9)$$

where $(\cdot)^H$, $\sigma_I^2$, and $\sigma_n^2$ denote the Hermitian transpose, the average received interference power, and the noise power, respectively. The power $\sigma_I^2$ and $\sigma_n^2$ are respectively given by

$$\begin{cases}\sigma_I^2=E\left[\sum_{c=1}^{6}\sum_{u=0}^{U-1}\left|\widetilde{H}_{m,u(c)}(k)\cdot S_{u(c)}(k)\right|^2\right] & \text{for } m=0\sim N_r-1,\\ \sigma_n^2=E\left[|n_m(t)|^2\right] & \text{for } m=0\sim N_r-1.\end{cases} \quad (10)$$

The detector output frequency-domain signal $\left\{\text{i.e., } \widetilde{\mathbf{S}}_0(k); k=0\sim N_c-1\right\}$ is transformed back by using $N_c$-point IFFT to the time-domain signal block $\left\{\text{i.e., } \widetilde{\mathbf{s}}(t); t=0\sim N_c-1\right\}$. The $u$-th element $\widetilde{s}_{u(0)}(t)$ of $\widetilde{\mathbf{s}}_0(t)$ is expressed as

$$\widetilde{s}_{u(0)}(t)=\frac{1}{N_c}\sum_{k=0}^{N_c-1}\widetilde{S}_{u(0)}(k)\exp\left(\frac{j2\pi kt}{N_c}\right), \quad (11)$$

where, $\widetilde{S}_{u(0)}(k)$ is the $u$-th element of $\widetilde{\mathbf{S}}_0(k)$. $\widetilde{s}_{u(0)}(t)$ is the decision variable. The symbol decision associated with the $u(0)$-th user is done as

$$\hat{s}_{u(0)}(t)=\arg\min_{s_{u(0)}\in D}\left|\widetilde{s}_{u(0)}(t)-s_{u(0)}(t)\right|, \quad (12)$$

where, $D$ is the symbol set given by (2) for QPSK modulation.

## IV. Simulation Results

### A. Simulation Procedure

Table 1 summarizes the simulation condition, and the flow chart of the computer simulation is illustrated in Fig. 4. The channel is assumed to be a frequency-selective block Rayleigh fading, having a symbol-spaced $L$-path uniform power delay profile.

First, $U$ users' locations are randomly generated in each cell for the given cluster size $N$. The path-loss and the log-normally distributed shadowing loss are generated for each user. Then $L$-path block Rayleigh fading associated with each user is generated. Signal transmission is simulated to measure the local average BER of the $U$ users in the $c$=0-th cell. This BER measurement is repeated a sufficient number of times by changing the user locations, and the complementary cumulative distribution function (CCDF) of the local average BER is obtained. The outage probability is the probability that the local average BER exceeds the required BER. If the outage probability is less than the allowable outage probability $Q$, the number $U$ of users is incremented by one. We define the link capacity as the maximum number $U_{\max}$ of supportable users normalized by the cluster size $N$. In this paper, we set the required BER and the allowable outage probability to $10^{-3}$ and 0.1, respectively.

As a benchmark comparison, we consider signal transmission using MMSE-FDE+antenna diversity reception [11]. In this method, the diversity combiner output and the weight vector are expressed as

$$\begin{cases}\widetilde{\mathbf{S}}_0(k)=\mathbf{Y}(k)^T\cdot\mathbf{w}(k)\\ \mathbf{w}(k)=\dfrac{\widetilde{\mathbf{H}}_{u(0)}^*(k)}{\left\|\widetilde{\mathbf{H}}_{u(0)}(k)\right\|^2+\dfrac{\sigma_I^2+\sigma_n^2}{P}}\end{cases}, \quad (13)$$

where $\|\cdot\|$ and $\widetilde{\mathbf{H}}_{u(0)}(k)=\left[H_{0,u(0)}\ \cdots\ H_{N_r-1,u(0)}\right]^T$ denote the Frobenius norm and the $u$-th column vector of $\widetilde{\mathbf{H}}_0(k)$ (see (5)), respectively.

### B. Uplink Capacity

Fig. 5 illustrates the CCDF of the local average BER for the case of $L$=16, $U$=4 and $N$=12 when $N_r$=8. From this figure, we notice that MMSED gives the lowest probability that the local average BER drops followed by the ZF that achieves almost the same probability. However, since MMSE-FDE+antenna diversity is a single-user detection, therefore the BER is very poor due to large multi-user interference.

Figs. 6 and 7 illustrate the uplink capacity i.e., $U_{\max}/N$ as a function of the cluster size value $N$ for $N_r$=4 and 8, respectively. First, we discuss the case of $N_r$=4 (see Fig. 6). MMSE-FDE+antenna diversity reception can only accommodate one user (i.e., $U_{\max}$=1). When the channel is frequency-nonselective ($L$=1), the cluster size maximizing the link capacity is $N$=9 (i.e., $U_{\max}/N$=0.111) for MMSE-FDE+antenna diversity reception. It can be seen that ZFD and MMSED can accommodate only one user and provide the same link capacity as MMSE-FDE+antenna diversity reception. Although multi-user MIMO multiplexing with MMSED can accommodate two users at $N$=19, the link capacity is then smaller than that at $N$=9.

When the channel is strongly frequency-selective ($L$=16), the cluster size that can maximize the link capacity is equal to $N$=7 (i.e., $U_{\max}/N$=0.143) for MMSE-FDE+antenna diversity reception. The maximum link capacity of ZFD and MMSED is slightly larger than that of MMSE-FDE+antenna diversity reception. It is equal to $U_{\max}/N$=0.166 (at $N$=12) for MMSED, and equal to $U_{\max}/N$=0.154 (at $N$=13) for ZFD. The achievable maximum link capacity in a frequency-selective channel is larger than that in frequency-nonselective channel. The link capacity achievable with MMSED in an $L$=16-path channel is almost 1.5 times larger than that in an $L$=1-path channel. This is due to the frequency diversity gain obtained by FDE.

Next, we discuss the case of $N_r$=8 (see Fig. 7). The link capacity of $N_r$=8 is larger than that of $N_r$=4. For an $L$=1-path channel, the cluster size that can maximize the link capacity is $N$=4 (i.e., $U_{\max}/N$=0.25) for MMSE-FDE+antenna diversity reception. MMSED achieves $U_{\max}/N$=0.286 at $N$=7. However, this is almost the same as the link capacity of MMSE-FDE+antenna diversity reception. On the other hand, for an $L$=16-path channel, multi-user MIMO multiplexing using ZFD or MMSED provides almost 1.3 times larger link capacity ($U_{\max}/N$=0.333 at $N$=9) than MMSE-FDE+antenna diversity reception ($U_{\max}/N$=0.25 at $N$=4).

From the above simulation results, it can be noticed that the frequency-selective channel helps to increase the link capacity and also multi-user MIMO multiplexing is only useful if many antennas (e.g., $N_r$=8) are employed at the BS.

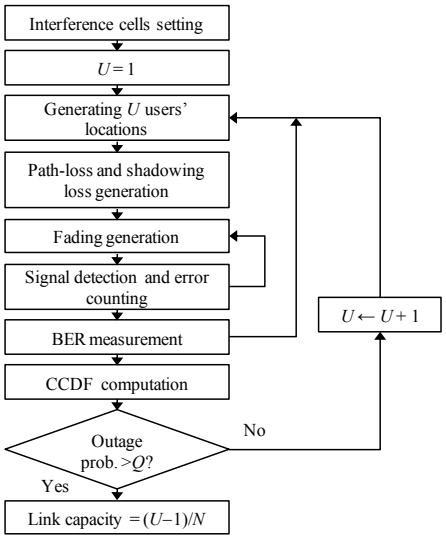


Figure 4. Flow chart of computer simulation.

Table 1. Simulation condition

| | | |
|---|---|---|
| Transmitter | Data modulation | QPSK |
| | Number of users per cell | $U$=1~6 |
| | FFT block size | $N_c$=256 |
| | GI length | $N_g$=32 |
| Channel | Path-loss exponent | $\alpha$=3.5 |
| | Standard deviation of shadowing loss | $\sigma$=7.0[dB] |
| | Fading | Block Rayleigh fading ($L$=1,16) |
| | Delay profile | Uniform |
| | Time delays | $\tau_l=lT_s$, $l$=0~$L$-1 |
| | Average received $E_b/N_0$ at the cell edge | 10dB |
| Receiver | Number of receive antennas | $N_r$=4 and 8 |
| | Signal detection | ZF and MMSE |
| | Channel estimation | Ideal |
| Required quality | Required BER | $10^{-3}$ |
| | Allowable outage probability | $Q$=0.1 |

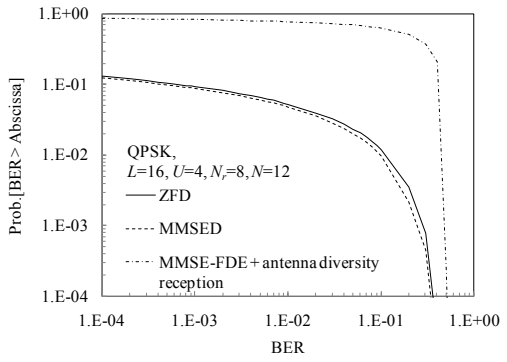


Figure 5. Complimentary cumulative distribution in terms of local average BER.

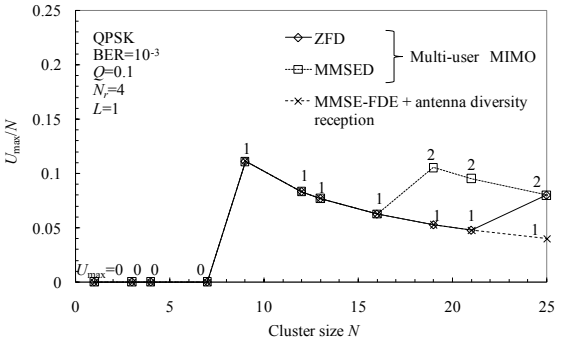


(a) $L$=1

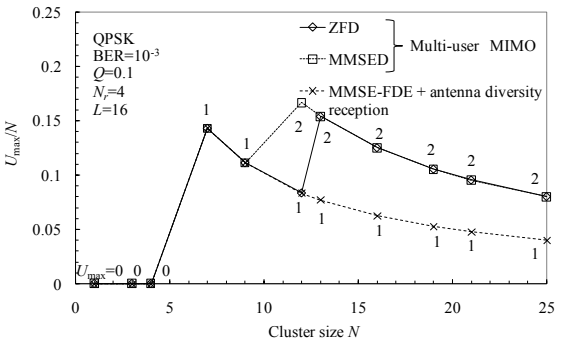


(b) $L$=16

Figure 6. Uplink capacity of multi-user MIMO multiplexing using 4-element antenna array.

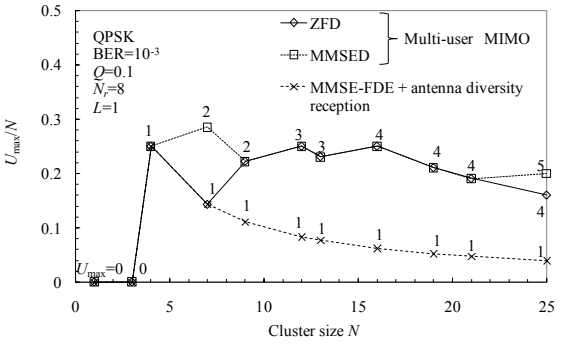


(a) $L$=1

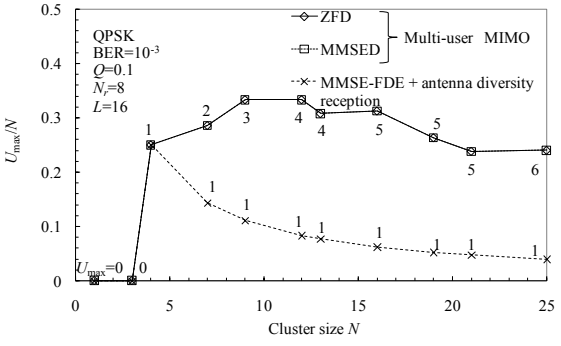


(b) $L$=16

Figure 7. Uplink capacity of multi-user MIMO multiplexing using 8-element antenna array.

## V. CONCLUSIONS

In this paper, we evaluated, by computer simulation, the uplink capacity of multi-user SC-MIMO multiplexing with frequency-domain equalization (FDE) using ZFD and MMSED in both frequency-selective and frequency-nonselective environment in a cellular system. From computer simulation result, it was shown that the frequency-selective channel helps to increase the uplink capacity. Both ZFD and MMSED provide almost the same link capacity and can achieve about 1.3 times larger uplink capacity than MMSE-FDE+antenna diversity reception when $N_r$=8. This suggests that the computationally efficient ZFD can be used instead of MMSED.

## REFERENCES

[1] F. Adachi, "Wireless past and future-evolving mobile communications systems," *IEICE Trans. Fundamentals*, Vol.E84-A, No.1, pp.55-60, Jan. 2001.

[2] John G. Proakis, *Digital Communications*, 4th edition, McGraw-Hill, 2001.

[3] G. L. Stüber, J. R. Barry, S. W. McLaughlin, Ye Li, M. A. Ingram, and T. G. Pratt, "Broadband MIMO-OFDM wireless communications," *Proc. IEEE*, Vol.92, No.2, pp.271-294, Feb. 2004.

[4] D. Falconer, S. L. Ariyavistakul, A. Benyamin-Seeyer, and B. Eidson, "Frequency domain equalization for single-carrier broadband wireless systems," *IEEE Commun. Mag*., Vol. 40, No. 4, pp. 58-66, Apr. 2002

[5] F. Adachi, D. Garg S. Takaoka, and K. Takeda, "Broadband CDMA techniques," Special Issue on Modulation, Coding and Signal Processing, *IEEE Wireless Commun. Mag.*, Vol.12, No. 2, pp. 8-18, Apr. 2005.

[6] H. Ekstrom, A. Furuskar, J. Karlsson, M. Meyer, S. Parkvall, J. Torsner, and M. Wahlqvist, "Technical solutions for the 3G long-term evolution," *IEEE Commun. Mag*., Vol.44, No.3, pp.38-45, Mar. 2006.

[7] Q.H.Spencer, C. B. Peel, A. L. Swindlehurst, and M. Haardt, "An Introduction to the multi-user MIMO downlink," *IEEE Commun. Mag.*, Vol.42, No.10, pp.60-67, Oct. 2004.

[8] W. C. Jakes, Jr., ed., *Microwave Mobile Communications*, John Wiley & Sons, New York, 1974.

[9] Y. Xie and C. N. Georghiades, "Some results on the sum-rate capacity of MIMO fading broadcast channels," *IEEE Trans. Wireless Commun*. Vol.5, No.2, pp.377-383, Feb. 2006

[10] G. Caire and S. Shamai, "On the achievable throughput of a multiantenna Gaussian broadcast channel," *IEEE Trans. Info. Theory,* Vol.49, No.7, pp.1691-1706, July 2003.

[11] F. Adachi and T. Sao, "Joint antenna diversity and frequency-domain equalization for multi-rate MC-CDMA," *IEICE Trans. Commun.*, Vol. E86-B, No. 11, pp. 3217–24, Nov. 2003.